Study of η' formation in photon-photon collisions

H. Aihara,[n] M. Alston-Garnjost,[a] R. E. Avery,[a] A. Barbaro-Galtieri,[a] A. R. Barker,[g] A. V. Barnes,[a] B. A. Barnett,[j] D. A. Bauer,[g] H. -U. Bengtsson,[d] D. L. Bintinger,[f] G. J. Bobbink,[h] T. S. Bolognese,[a] A. D. Bross,[a] C. D. Buchanan,[d] A. Buijs,[m] D. O. Caldwell,[g] A. R. Clark,[a] G. D. Cowan,[a] D. A. Crane,[j] O. I. Dahl,[a] K. A. Derby,[a] J. J. Eastman,[a] P. H. Eberhard,[a] T. K. Edberg,[a] A. M. Eisner,[c] R. Enomoto,[n] F. C. Erné,[m] T. Fujii,[n] J. W. Gary,[a] W. Gorn,[e] J. M. Hauptman,[i] W. Hofmann,[a] J. E. Huth,[a] J. Hylen,[j] T. Kamae,[n] H. S. Kaye,[a] K. H. Kees,[f] R. W. Kenney,[a] L. T. Kerth,[a] Winston Ko,[b] R. I. Koda,[d] R. R. Kofler,[k] K. K. Kwong,[e] R. L. Lander,[b] W. G. J. Langeveld,[e] J. G. Layter,[e] F. L. Linde,[m] C. S. Lindsey,[e] S. C. Loken,[a] A. Lu,[g] X-Q. Lu,[j] G. R. Lynch,[a] R. J. Madaras,[a] K. Maeshima,[b] B. D. Magnuson,[c] J. N. Marx,[a] G. E. Masek,[f] L. G. Mathis,[a] J. A. J. Matthews,[j] S. J. Maxfield,[k] S. O. Melnikoff,[e] E. S. Miller,[f] W. Moses,[a] R. R. McNeil,[b] P. Nemethy,[l] D. R. Nygren,[a] P. J. Oddone,[a] H. P. Paar,[m] D. A. Park,[d] S. K. Park,[i] D. E. Pellett,[b] M. Pripstein,[a] M. T. Ronan,[a] R. R. Ross,[a] F. R. Rouse,[a] K. A. Schwitkis,[g] J. C. Sens,[m] G. Shapiro,[a] M. D. Shapiro,[a] B. C. Shen,[e] W. E. Slater,[d] J. R. Smith,[b] J. S. Steinman,[d] M. L. Stevenson,[a] D. H. Stork,[d] M. G. Strauss,[d] M. K. Sullivan,[c] T. Takahashi,[n] J. R. Thompson,[f] N. Toge,[n] S. Toutounchi,[k] R. van Tyen,[a] B. van Uitert,[m] G. J. VanDalen,[e] R. F. van Daalen Wetters,[d] W. Vernon,[f] W. Wagner,[b] E. M. Wang,[a] Y. X. Wang,[g] M. R. Wayne,[d] W. A. Wenzel,[a] J. T. White,[f] M. C. S. Williams,[b] Z. R. Wolf,[a] H. Yamamoto,[a] S. J. Yellin,[g] C. Zeitlin,[b] and W-M. Zhang[j]

[a]*Lawrence Berkeley Laboratory, Berkeley, California 94720*

[b]*University of California, Davis, California 95616*

[c]*University of California Intercampus Institute for Research at Particle Accelerators, Stanford, California 94305*

[d]*University of California, Los Angeles, California 90024*

[e]*University of California, Riverside, California 92521*

[f]*University of California, San Diego, California 92093*

[g]*University of California, Santa Barbara, California 93106*

[h]*Carnegie-Mellon University, Pittsburgh, Pennsylvania 15213*

[i]*Ames Laboratory, Iowa State University, Ames, Iowa 50011*

[j]*Johns Hopkins University, Baltimore, Maryland 21218*

[k]*University of Massachusetts, Amherst, Massachusetts 01003*

[l]*New York University, New York, New York 10003*

[m]*National Institute for Nuclear and High Energy Physics, Amsterdam, The Netherlands*

[n]*University of Tokyo, Tokyo, Japan*

(TPC/Two-Gamma Collaboration)

(Received 15 December 1986)

Two-photon formation of the η' in the reaction $e^+e^-\to e^+e^-\eta'\to e^+e^-\pi^+\pi^-\gamma$ has been studied for nearly real and virtual photons at an e^+e^- center-of-mass energy of 29 GeV. The $\gamma\gamma$ width of the η' is found to be 4.5 ± 0.3(stat.)±0.7(syst.) keV. The measured dependence of this $\gamma\gamma$ width upon the photon four-momentum squared in the range 0—5 GeV^2 agrees with predictions both from QCD and from ρ dominance. A spin analysis results in a strong preference for a spin-zero, relative to a spin-two, assignment for the η'. No evidence for C-parity violation is found in this $\eta'\to\pi^+\pi^-\gamma$ decay mode.

The study of resonance formation in photon-photon collisions is of interest because it can provide a determination of the charged-parton content of the resonance from its two-photon width.[1] The determination of the quark content of the η and η' is especially important, since the breakdown of the Gell-Mann—Okubo mass formula for pseudoscalar particles, as opposed to its success for vector particles, has been interpreted as possible evidence for gluon content in the η or η' (Ref. 2). In addition, the dependence of the two-photon width for pseudoscalar mesons upon the four-momentum squared (q^2) of the virtual photon has been predicted by a QCD model.[3] Several recent experiments have yielded a range of values for the two-photon width of the η' at $q^2=0$, $\Gamma_{\gamma\gamma}(\eta')$, from 3.8 to 6.2 keV (Refs. 4—8). Here we report our measurements of this width and its q^2 dependence.

The data were obtained at the SLAC e^+e^- storage ring PEP, operating at 29-GeV center-of-mass energy, by ob-

serving the reaction $e^+e^- \to e^+e^-\eta' \to e^+e^-\rho\gamma \to e^+e^-\pi^+\pi^-\gamma$ in the TPC/Two-Gamma detector. The apparatus is described elsewhere,[9] but features relevant to this analysis are mentioned here. The Time Projection Chamber (TPC), in a 0.4-T solenoidal magnetic field, had a momentum resolution of $(\sigma_p/p)^2 = 0.06^2 + (0.035p/\text{GeV})^2$. Charged particles in the central detector were identified by measuring ionization loss (dE/dx). In the forward direction, charged particles were tracked in two spectrometers, each containing 15 drift-chamber planes and a septum magnet ($\int B\,dl = 0.24$ T m). Electrons, positrons, and photons were detected by NaI counters (with the polar angle θ between 24 and 90 mrad), lead-scintillator shower counters ($100 < \theta < 180$ mrad), lead—proportional-chamber pole-tip calorimeters (PTC's) ($250 < \theta < 660$ mrad) and, at larger polar angles, by a lead Geiger-mode hexagonal calorimeter (HEX) placed outside the solenoid. There were cylindrical drift chambers at the inner radius of the TPC (IDC) and outside the solenoid (ODC).

Data used in this investigation were logged with two independent triggers. A tagged trigger required the coincidence of an energy deposition in one of the forward calorimeters (a tag) with either an indication of charge in the central drift chambers or an energy deposit in the HEX or PTC. An untagged trigger required at least two TPC tracks, each with hits in the IDC and either the ODC or the TPC end plane. For the untagged trigger, the TPC tracks had to be in different 60° azimuthal sectors, with polar angles greater than 30° from the beam, and had to project back to the vertex to within 20 cm along the beam line. The untagged and tagged event samples correspond to integrated luminosities of 74 and 50 pb^{-1}, respectively.

In the analysis, we selected events with two oppositely charged particles and one photon (not counting a tag). For the untagged sample, both charged particles were required to be identified as pions by dE/dx within the TPC fiducial volume and to extrapolate to within 5 cm of the interaction point along the beam line. The single-tagged analysis required only one of the two charged particles to be identified by the TPC, matching the looser trigger definition. Further cuts were needed to reduce backgrounds from cosmic-ray muons and e^+e^- annihilation, as well as from other two-photon topologies such as exclusive two-prong and nonexclusive events. For the untagged data, these cuts were visible energy < 11.6 GeV, missing $p_\perp < 0.6$ GeV, $\pi\pi$ transverse momentum $|\mathbf{p}_\perp(\pi^+) + \mathbf{p}_\perp(\pi^-)| > 0.04$ GeV, azimuthal angle $|\phi(\pi^+) - \phi(\pi^-)| < 3.05$ rad, and $|\phi(\pi^+\pi^-) - \phi(\gamma)| > 1.7$ rad. The only relevant background in the tagged data, from nonexclusive events, was suppressed by requiring missing $p_\perp < 0.6$ GeV and $|\cos\theta_\pi^{**}| < 0.75$, where θ_π^{**} is the decay angle of a π in the ρ-helicity frame. Single-tagged events were required to have a tag, defined as a charged track in the forward drift chambers which points to an energy deposition greater than 5 GeV in the NaI or greater than 10 GeV in the lead-scintillator detector. For the untagged sample, the final-state photon was required to be in the pole tip or the hexagonal calorimeters and have a measured energy greater than 100 or 70 MeV, respectively. For the tagged sample, the photon could also have been in the NaI or lead-scintillator detector, with energy greater than 300 or 500 MeV, respectively.

The events which passed these cuts were then kinematically fitted to an $ee\pi\pi\gamma$ final state. The average photon energies of the η' decays in this experiment, ≈ 250 (500) MeV for the untagged (tagged) data, are difficult to measure accurately in our apparatus. Thus, much larger uncertainties were assigned to the photon energy than to the other kinematic quantities in the fit. Events were kept which had a confidence level for the fit of at least 5% and a fitted photon energy greater than 100 MeV. After these cuts, 1658 (213) events were left in the untagged (tagged) sample. For the untagged events, 30% pass the confidence level and photon energy cuts compared to 77% for η' generated by a Monte Carlo simulation to be described below. The difference is largely accounted for by background events. An alternative method of analysis[10] relied upon tighter $p_\perp$-balance cuts to reject much of the nonexclusive background before presenting it to the fit. With these cuts, 84% of the data and 97% of the Monte Carlo events passed the confidence-level and photon-energy cuts. Nevertheless, the acceptance-corrected η' yield agreed with that from the first method to within 1%. An analogous test[11] on the single-tag events led to a similar conclusion.

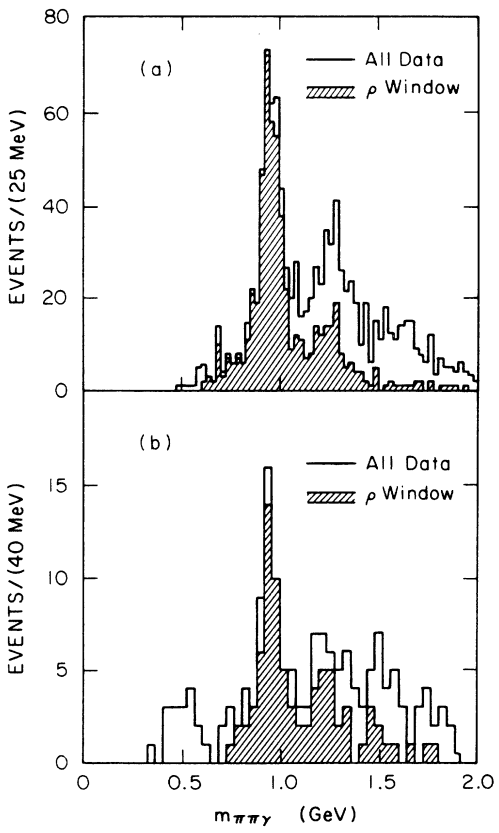

FIG. 1. $\pi\pi\gamma$ mass spectra for untagged (a) and single-tagged (b) events. Histograms are shown for kinematically fitted quantities, with and without a window on the $\pi\pi$ mass around the ρ.

Figure 1 shows the $\pi\pi\gamma$ mass spectra, untagged and tagged, with and without a window on the $\pi\pi$ mass around the ρ (500—850 MeV). A clear $\eta'(958)$ signal is seen, with a background under the peak of about 20%. One also sees the A_2 [$a_2(1320)$] through its decay mode $A_2\to\pi^+\pi^-\pi^0$, with one of the two photons from the π^0 decay undetected. In Fig. 2 we give the $\pi\pi$ mass spectra, again untagged and tagged, with a window on the $\pi\pi\gamma$ mass around the η' (880—1040 MeV). Clearly most of the events are in the ρ mass region.

To determine the acceptance, events were generated in a Monte Carlo program based on the $\gamma\gamma$ luminosity function of Ref. 12 and on the matrix element $i\sqrt{X}F_{\eta'}(q_1^2,q_2^2)$ defined in Ref. 13 for the production of a pseudoscalar η' by two virtual photons. Here $X=(q_1\cdot q_2)^2-q_1^2q_2^2$, with q_i the photon four-momenta and $F_{\eta'}$ the form factor; at $q_1^2=q_2^2=0$ one has (from the definition of Γ) $F^2(0,0)=64\pi\Gamma_{\gamma\gamma}/m_{\eta'}^3$. The cross section for $\gamma^*\gamma^*\to\eta'$ is

$$\sigma_{\gamma^*\gamma^*\to\eta'}=\frac{\pi}{4}\sqrt{X}F^2(q_1^2,q_2^2)\delta(W_{\gamma^*\gamma^*}^2-m_{\eta'}^2)\ , \quad (1)$$

with $W^2=(q_1+q_2)^2$ the $\gamma\gamma$ c.m. energy squared. For the q^2 dependence of F, the Monte Carlo simulation used form factors from ρ dominance,

$$F^2(q_1^2,q_2^2)=\frac{64\pi\Gamma_{\gamma\gamma}}{m_{\eta'}^3}\left[\frac{1}{1-q_1^2/m_\rho^2}\right]^2\left[\frac{1}{1-q_2^2/m_\rho^2}\right]^2, \quad (2)$$

consistent with the q^2 dependence reported below. Note that one of the virtual photons is nearly real ($q_i^2\approx 0$) in this single-tagged reaction. For the decay $\eta'\to\rho\gamma\to\pi^+\pi^-\gamma$, we have used

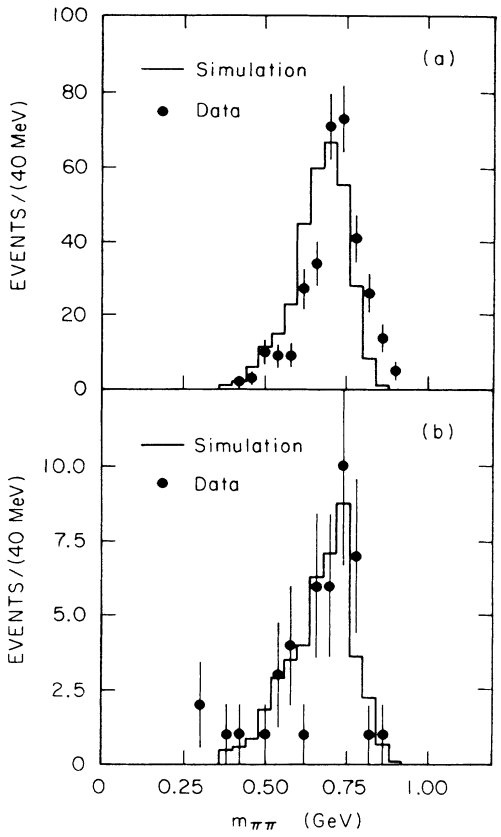

FIG. 2. $\pi\pi$ effective-mass spectra, after kinematic fitting, for untagged (a) and single-tagged (b) events. Shown are data and Monte Carlo simulations.

$$\Gamma\propto k^{*3}\left[\frac{m_\rho\Gamma_\rho(m_{\pi\pi})dm_{\pi\pi}^2}{(m_\rho^2-m_{\pi\pi}^2)^2+m_\rho^2\Gamma_\rho^2(m_{\pi\pi})}\right]\sin^2\theta_\pi^{**}d\Omega_\pi^{**}d\Omega_\gamma^*\ . \quad (3)$$

Here k^* and Ω_γ^* are the energy and solid angle of the photon in the η' center of mass, with θ_π^{**} and Ω_π^{**} the polar and solid angles of the π^+ in the ρ-helicity frame. Also, $m_{\pi\pi}$ is the $\pi\pi$ effective mass and m_ρ is the nominal mass of the ρ [770±3 MeV (Ref. 14)]. The radiative transition $\eta'\to\rho\gamma$ is a pure magnetic dipole transition ($\Delta J=1$, no parity change). Higher-order transitions are forbidden by parity and angular momentum conservation. The $\sin^2\theta_\pi^{**}$ angular distribution is characteristic for decay of an aligned vector meson of helicity ±1. The expression in large parentheses is an energy-dependent Breit-Wigner distribution which should account for the relatively large width of the ρ. We used[15] $\Gamma_\rho(m_{\pi\pi})=\Gamma_\rho^0(q^{**}/q_0^{**})^3(m_\rho/m_{\pi\pi})$, with Γ_ρ^0 the nominal width of the ρ [153±2 MeV (Ref. 14)], q^{**} the momentum of a π in the ρ helicity frame, and $q_0^{**}=q^{**}$ for $m_{\pi\pi}=m_\rho$. The small shift between the data and Monte Carlo $\pi\pi$ mass spectra seen in Fig. 2 is probably due to the difficulty in modeling decays involving a broad resonance such as the ρ.

The major sources of uncertainty in the event simulation are the trigger efficiency in the untagged data and the detection efficiency for photons in the calorimeters. The trigger efficiency was determined from a Monte Carlo simulation of the trigger hardware, with input from independently triggered data on the probabilities for particles to reach the outer drift chamber as a function of $p_\perp$ and θ. Differences in efficiency between π^+ and π^- were found to be negligible. Photon detection efficiencies were derived, separately for each calorimeter, from the measured detection efficiencies for electrons and positrons. The intrinsic efficiency of each calorimeter was assumed to be the same for photon and $e^\pm$ induced showers. The EGS code[16] was then used to correct for the difference in the propagation of $e^\pm$ and photons through the material in front of the calorimeters. HEX and PTC photon efficiencies were found to be similar, rising from nearly 0 for produced photon energies less than 100 MeV to at least 90% for energies greater than 400 MeV (Ref. 11).

The untagged data sample within the ρ window in Fig. 1(a) was fitted to the sum of an η' Gaussian peak, a

Breit-Wigner form for the A_2, and a third-degree polynomial for the background. This leads to a $\gamma\gamma$ width $\Gamma_{\gamma\gamma}(\eta')=4.5\pm0.3$ keV, where the error is statistical and we have used the nominal value for the branching ratio $B(\eta'\to\rho\gamma)$ (Ref. 14) of 0.30. A 0.7-keV (15%) systematic uncertainty is assigned to this width due to uncertainties in the background shape (5%), trigger efficiency (5%), photon detection efficiency (10%), fit efficiency (5%), luminosity (5%), and branching ratio $B(\eta'\to\rho\gamma)$ (5%). The values of $\Gamma_{\gamma\gamma}(\eta')$ for events with photons in the HEX or PTC are 4.2 ± 0.4 keV and 4.9 ± 0.6 keV, respectively (errors are statistical only). These two values are consistent with each other, especially when their systematic errors are taken into account. Table I shows results of this and other recent experiments for the $\gamma\gamma$ width of the η' at $q^2=0$. The inclusion of our measurement with the present world-average value[14] gives $\Gamma_{\gamma\gamma}(\eta')=4.48\pm0.35$, where the statistical and systematic errors have been added in quadrature.

The single-tagged data sample within the ρ window in Fig. 1(b) was fitted in a way similar to that of the untagged sample, but in five separate bins of $Q^2=-q^2$ of the tagged photon. A 14% systematic error in the single-tagged data comes from uncertainties in the background shape (10%), trigger efficiency (3%), photon detection efficiency (4%), fit efficiency (5%), luminosity (4%), and branching ratio (5%). Figure 3 shows $m_{\eta'}^3F^2/64\pi$ as a function of Q^2, together with the untagged $Q^2=0$ point. The dotted curve is a QCD prediction for the Q^2 dependence of the η' form-factor squared.[3] Also shown are curves for ρ and ϕ dominance. The data are seen to agree with both QCD and ρ dominance but not with ϕ dominance. The Q^2 dependence agrees with an earlier determination[5] made in the smaller range $0<Q^2<1$ GeV^2.

The quark and gluon content of the η' can be determined using Rosner's analysis,[1] which relies upon the assumptions of SU(3) and nonet symmetry, among others. One defines

$$|\eta'\rangle=\frac{x}{\sqrt{2}}(|u\bar{u}\rangle+|d\bar{d}\rangle)+y\,|s\bar{s}\rangle+z\,|G\rangle\ ,$$

with G a neutral-parton (gluon) content. Using the average value for $\Gamma_{\gamma\gamma}(\eta')=4.48\pm0.35$ described above, and the known[14] branching ratios of η' to $\gamma\gamma$ and $\rho\gamma$, we can calculate $\Gamma(\eta'\to\rho\gamma)$. From this and the current world average for $\Gamma(\omega\to\pi^0\gamma)$ (Ref. 14), Eq. (17) of Ref. 1 gives $|x|=0.57\pm0.04$. Using this value of x and the present world average for $\Gamma_{\gamma\gamma}(\pi^0)$ (Ref. 14), Eq. (22) of Ref. 1 yields $|y|=0.75\pm0.13$. Thus $x^2+y^2=0.89\pm0.17$, leaving a possible gluon content, $z^2=0.11\pm0.17$ in the η'. Reducing the uncertainty in these values will require more precise measurements for $\Gamma(\omega\to\pi^0\gamma)$ and $\Gamma_{\gamma\gamma}(\pi^0)$, as well as for $\Gamma_{\gamma\gamma}(\eta')$. Note that the relatively large fraction of strange quarks in the η' does not seem to shift the measured Q^2 dependence (Fig. 3) towards a ϕ form factor. The Mark III Collaboration[17] has obtained values for the quark content of the η' of $|x|=0.36\pm0.05$ and $|y|=0.72\pm0.12$ by using measurements of the decays $J/\psi\to\omega\eta'$ and $J/\psi\to\rho\eta'$. The disagreement in $|x|$ values between the two-photon measurements and those from the J/ψ decays may reflect a breakdown in one or more of the theoretical assumptions used in this type of analysis.[18]

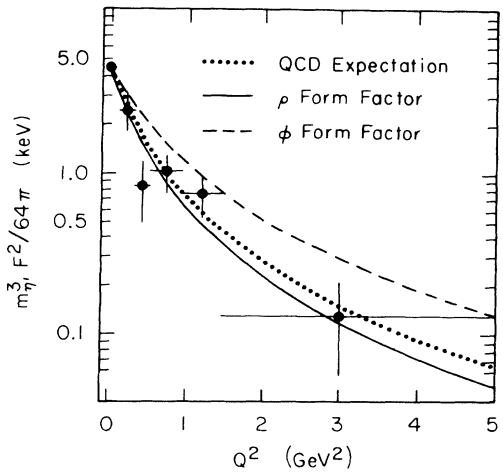

FIG. 3. $m_{\eta'}{}^3F^2/64\pi$ as a function of Q^2. The $Q^2=0$ point is $\Gamma_{\gamma\gamma}(\eta')$. The vertical error bars indicate the 65%-confidence limits based upon statistical errors only. The curves shown are the expectations from QCD (Ref. 3), ρ dominance, and ϕ dominance.

The reaction $\gamma\gamma\to\eta'\to\rho\gamma$ provides a sensitive measure of the η' spin because the γ helicity results in a spin alignment for the η' (for $J\neq0$) as well as for the ρ. Previous spin determinations of the η' from Dalitz-plot analyses of $\eta'\to\pi\pi\eta$ or $\eta'\to\pi\pi\gamma$ in hadronic production[14] favored spin zero, but did not completely rule out spin two. In Fig. 4(a) and 4(b) we show two decay distributions: $\cos\theta_\gamma^*$ (with θ_γ^* the polar angle of the photon in the η' center of mass) and $\cos\theta_\pi^{**}$, respectively, with the windows on the $\pi\pi\gamma$ and $\pi\pi$ masses as defined earlier. The solid curves

TABLE I. $\Gamma_{\gamma\gamma}(\eta')$ as determined by recent experiments. The statistical and systematic errors are shown separately.

Experiment	$\Gamma_{\gamma\gamma}(\eta')$ (keV)	Reference
TPC/Two-Gamma	$4.5\pm0.3\pm0.7$	This expt.
TASSO	$5.1\pm0.4\pm0.7$	4
PLUTO	$3.8\pm0.3\pm0.4$	5
CELLO	$6.2\pm1.1\pm0.8$	6
Mark II (SPEAR)	$5.8\pm1.1\pm1.2$	7
JADE	$5.0\pm0.5\pm0.9$	8

TABLE II. χ^2's obtained in fits of θ_γ^* and θ_π^{**} distributions for various spin and helicity hypotheses for the η'. There are 19 degrees of freedom in each fit. The last line in the table is for equal probabilities for helicities 0, +2, −2.

Spin	Helicity	$\chi^2(\theta_\gamma^*)$	$\chi^2(\theta_\pi^{**})$
0	0	16.2	20.7
2	0	53.6	30.6
2	±2	26.6	68.4
2	0, ±2	22.8	52.8

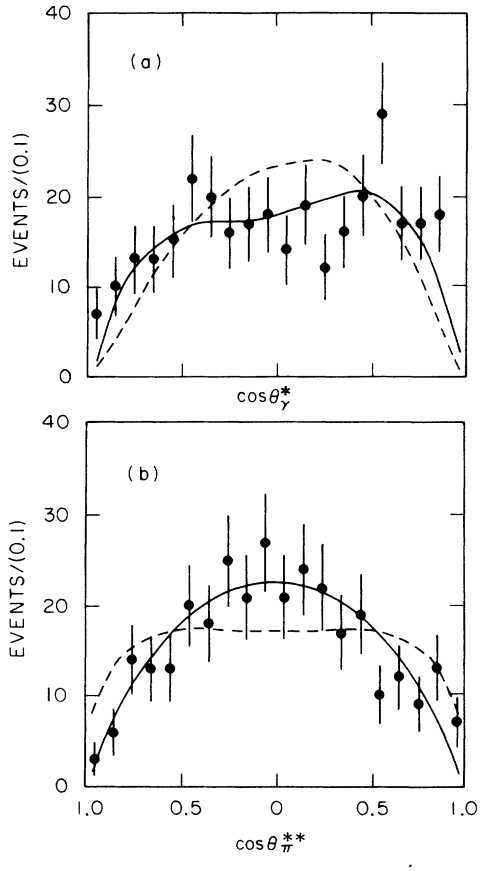

FIG. 4. Distributions for (a) $\cos\theta_\gamma^*$ and (b) $\cos\theta_\pi^{**}$ for $J^P=0^-$ (solid curves) and 2^- (dashed curves) Monte Carlo fits to the data. The dashed curves are for equal helicities $0, +2, -2$.

are the Monte Carlo predictions for spin zero, using Eq. (3); the dashed curves are the predictions for spin two using a modified Eq. (3) and assuming equal probabilities for helicities $0, +2$, and -2 (Ref. 10). The spin-zero curves are seen to fit the data better than those for spin two. More quantitatively, we give in Table II the χ^2's for the fits of the expected θ_π^{**} and θ_γ^* dependences of the decay rate. It is evident that the spin-zero hypothesis gives a good fit to the data, while spin two is rejected by the χ^2 of either the θ_γ^* or the θ_π^{**} fits. We find that, for any combination of helicities 0 and ± 2, the confidence level for the spin-two hypothesis, relative to that of the spin-zero hypothesis, is 2×10^{-4} or less.

If a C-parity-violating interaction of strength comparable to that of the electromagnetic interaction should occur in nature, the electromagnetic decays of the η' would show observable interference effects. In particular, the $\eta'\to\pi\pi\gamma$ decays studied in this experiment would have a forward/backward asymmetry in the θ_π^{**} distribution. From Fig. 4(b), we have measured this asymmetry to be $(-1.9\pm 5.6)\%$. Furthermore, the shape of the θ_π^{**} distribution is inconsistent with what would be expected if a C-parity-violating interaction were dominant. At the 95% confidence level, we find no more than a 9% admixture of a C-parity-violating amplitude with the C-parity-conserving one. These results strongly favor the hypothesis of C-parity conservation and agree with those of other experiments.[19]

In summary, our measurement of the $\gamma\gamma$ width of the η' at $Q^2=0$ agrees well with values from other experiments. These measurements can be used to obtain information on the parton content of the η'. We have also studied the Q^2 dependence of the width, finding it consistent with both QCD and ρ-dominance predictions. A spin-parity Dalitz analysis confirms the pseudoscalar nature of the η', with no evidence for charge-conjugation-parity violation.

We gratefully acknowledge the efforts of the PEP staff and the engineers, programmers, and technicians of the collaborating institutions. This work was supported in part by the United States Department of Energy, the National Science Foundation, the Joint Japan-United States Collaboration in High Energy Physics, and the Foundation for Fundamental Research on Matter in The Netherlands.

[1]J. L. Rosner, Phys. Rev. D **27**, 1101 (1983).
[2]R. Friedberg and T. D. Lee, Phys. Rev. D **18**, 2623 (1978), and references therein.
[3]S. J. Brodsky and G. P. Lepage, Phys. Rev. D **24**, 1808 (1981).
[4]M. Althoff *et al.*, Phys. Lett. **147B**, 487 (1984).
[5]Ch. Berger *et al.*, Phys. Lett. **142B**, 125 (1984).
[6]H. J. Behrend *et al.*, Phys. Lett. **114B**, 378 (1982); **125B**, 518(E) (1983).
[7]G. S. Abrams *et al.*, Phys. Rev. Lett. **43**, 477 (1979); P. Jenni *et al.*, Phys. Rev. D **27**, 1031 (1983).
[8]W. Bartel *et al.*, Phys. Lett. **113B**, 190 (1982).
[9]H. Aihara *et al.*, I.E.E.E. Trans. Nucl. Sci. **NS30**; 63 (1983); **NS30**, 67 (1983); **NS30**, 76 (1983); **NS30**, 117 (1983); **NS30**, 153 (1983); **NS30**, 162 (1983); M. P. Cain *et al.*, Phys. Lett. **147B**, 232 (1984).
[10]Bert Van Uitert, Ph.D. thesis, State University of Utrecht, The Netherlands, 1986.
[11]Kent Schwitkis, Ph.D. thesis, University of California, Santa Barbara, 1986.
[12]V. E. Balakin, V. M. Budnev, and I. F. Ginzburg, Pis'ma Zh. Eksp. Teor. Fiz. **11**, 559 (1970) [JETP Lett. **11**, 388 (1970)]; G. Bonneau, M. Gourdin, and F. Martin, Nucl. Phys. **B54**, 573 (1973); V. M. Budnev *et al.*, Phys. Rep. **15C**, 181 (1975).
[13]G. Köpp, T. F. Walsh, and P. Zerwas, Nucl. Phys. **B70**, 461 (1974).
[14]Particle Data Group, M. Aguilar-Benitez *et al.*, Phys. Lett. **170B**, 1 (1986).
[15]J. D. Jackson, Nuovo Cimento **34**, 1644 (1964).
[16]R. L. Ford and W. R. Nelson, SLAC Report No. 210, 1978.
[17]R. M. Baltrusaitis *et al.*, Phys. Rev. D **32**, 2883 (1985).
[18]Stephen S. Pinsky, Phys. Rev. D **31**, 1753 (1985).
[19]A. Rittenberg *et al.*, Phys. Rev. Lett. **15**, 556 (1965); G. R. Kalbfleisch *et al.*, Phys. Rev. D **11**, 987 (1975); A. Grigorian *et al.*, Nucl. Phys. **B91**, 232 (1975).